

Periodic splay-twist Fréedericksz transition for nematics confined between two concentric cylinders

Giuseppe Bevilacqua

CNISM and Dipartimento di Fisica, Università di Siena, via Roma 56, 53100 Siena, Italy

Gaetano Napoli

Dipartimento di Ingegneria dell'Innovazione, Università del Salento, via per Monteroni, Edificio "Corpo O," 73100 Lecce, Italy

(Received 7 July 2009; published 22 March 2010)

This paper derives theoretical results for the periodic splay-twist Fréedericksz transition in nematic liquid crystals confined between two infinite concentric cylinders. The calculation of Lonberg and Meyer [Phys. Rev. Lett. **55**, 718 (1985)], for nematics sandwiched between two infinite planes, is extended to annular domains. The phase transition is triggered by an applied voltage between the outer and the inner delimiting walls. The critical threshold behavior is analyzed via the linearized Euler-Lagrange equations related to the Frank's free energy. It is found that, the threshold depends on both the ratio between the twist and the splay elastic constants, and the sample radii ratio. Results for planar samples are recovered in the thin cell limit. With respect to the planar geometry, our analysis predicts that for annular geometries the periodic Fréedericksz transition is also allowed for elastic anisotropies $K_2/K_1 > 0.303$.

DOI: [10.1103/PhysRevE.81.031707](https://doi.org/10.1103/PhysRevE.81.031707)

PACS number(s): 61.30.Dk, 61.30.Gd, 46.32.+x

I. INTRODUCTION

Nematic liquid crystals [1] are aggregates of rodlike molecules. The interaction between neighboring molecules tries to make them parallel to each other, and induces a partial ordering at mesoscopic scales. Early continuum theories [2–4] describe the nematic configurations through a unit vector \mathbf{n} , called the *director*, pointing along the average orientation. Within these theories, a local stored energy function depending on \mathbf{n} and its gradient is assumed. The director \mathbf{n} adjusts throughout the sample in order to minimize that energy according to the boundary conditions. The particular shape and structure makes the molecules very sensitive to the presence of electric or magnetic fields. Depending on their dielectric or diamagnetic properties, the molecules reorient along or normally to the direction of the field. Thus, the optical response of a cell containing nematics, which is related to the \mathbf{n} orientation, may be driven by the action of external fields. The controllable long range orientational response of nematics is crucial in designing of electro-optic devices.

The Fréedericksz transition is one of the most investigated effects in the physics of nematic liquid crystals, from both the fundamental and practical point of view. It is a second-order phase transition from a uniform director alignment to a distorted one, under the action of an external electric or magnetic field. This phenomenon, first observed by Fréedericksz and Zolina [5], can be explained as follows. Let us consider a nematic sandwiched between two parallel glasses. Delimiting surfaces can be treated in such a way that leads to an homogeneous planar orientation of the molecules at the boundary. Thus, an uniform alignment throughout the sample can be induced. In this scenario, an external field applied normally to the undistorted director field tends to reorient the molecules. This effect competes against both the elastic nematic behavior and the surface anchoring which hinder the molecular rotation. There is a critical field below which the

internal elastic strength of the liquid crystal exceeds the electric forces and hence the system remains undeformed. On the contrary, beyond this threshold the director field undergoes a static distortion, which usually is pure splay, or pure twist or pure bend, (see for example [6] and references therein). This kind of distortions are homogeneously distorted field-induced states: the nematic director depends only on the coordinate orthogonal to the delimiting walls and is homogeneous in the other directions. Nevertheless, it has been discovered by Lonberg and Meyer [7] that in polymeric nematic liquid crystals, a second-order phase transition to a periodic state, rather than homogeneous, occurs at a lower threshold than the usual Fréedericksz transition. Under strong planar anchoring boundary conditions, a magnetic field induces periodic stripes in the plane orthogonal to the initially undistorted molecules alignment. Such effect is called the splay-twist periodic Fréedericksz transition or briefly the periodic Fréedericksz transition (PFT) as opposed to the homogeneous Fréedericksz transitions (HFT) described above. Recent experimental studies [8–10] report as the PFT in nematics can be induced also by light fields.

An analysis of the PFT critical threshold performed via linearized equilibrium equations is reported in the pioneer paper [7] and presents good agreement with the experimental observation. The key feature of the new observed transition is the low ratio between the twist and the splay elastic constants, here denoted by κ , which is a consequence of the high length to width ratio of molecules. In fact, if the twist constant is small enough, the splay-twist distortion is energetically preferred respect to the pure splay one. The calculation of Lonberg and Meyer shows that both the critical threshold and the undulation wavelength depend on κ . In agreement with the experimental results reported in [7], Oldano [11] theoretically predicted that the PFT occurs unless κ does not exceed the critical value $\kappa_{pl}=0.30325$. Subsequent works [12,13] generalized the original analysis to weak anchoring boundary conditions.

Both HFT and PFT have been extensively studied in planar configuration. Williams and Halperin [15] first studied the configurations of a nematic liquid crystal confined between two concentric cylinders. They consider strong homeotropic conditions at the walls. Within this geometry the field-free configuration is already distorted. Denoted ρ the ratio of the outer and the inner cylinder radii, the director is purely radial for a ρ less than a certain ρ_{cr} . Otherwise the director *escapes into the third dimension* and gains an axial component [16]. This represents a kind of geometrically induced Fréedericksz-like transition. When combined with a radial field and a nematic liquid crystal with a negative dielectric anisotropy, the critical voltage of the Fréedericksz transition can be made arbitrarily small. A couple of subsequent works by Barratt and Duffy [17,18] consider six different arrangements covering all cases in which the (mutually orthogonal) external field and initial director field are either radial, azimuthal or axial, with possibility of weak anchoring conditions.

Inspired by the theoretical calculation of Lonberg and Meyer [7], we investigate the splay-twist Fréedericksz transition for nematics confined between two concentric cylinders. We consider a nematic whose molecules at walls are fixed in the direction of the cylinder axis. This means that in the free-field configuration the nematic is uniformly aligned along the same direction axis. Then we suppose that a voltage difference is applied between the delimiting walls and we look for periodic azimuthal solutions of the equilibrium equations. As in the planar geometry [7], we obtain that the PFT may occur at a critical threshold less than that expected for the HFT. However, in the annular geometry the critical threshold and the wavelength vector of the undulation depends on both κ and ρ . We show that the PFT is also allowed for values of κ greater than the limit established in the planar geometry, widening the class of nematics in which the PFT may be observed.

This paper is organized as follows. In Sec. II we write the free energy to minimize. In Secs. III and IV we derive and solve the Euler-Lagrange equations related to the free energy in the case of homogeneous and periodic distortions, respectively. The results of our analysis are presented in Sec. V. Some conclusions are pointed out in Sec. VI.

II. MODEL

Within the Frank's continuum theory of nematic liquid crystals, the elastic response of the material is characterized by a free energy per unit volume,

$$w_N = \frac{K_1}{2}(\text{div } \mathbf{n})^2 + \frac{K_2}{2}(\mathbf{n} \cdot \text{curl} \mathbf{n})^2 + \frac{K_3}{2}|\mathbf{n} \times \text{curl} \mathbf{n}|^2,$$

where K_1 , K_2 , and K_3 are positive constants. The three terms penalize in energy the splay, twist and bend distortion, respectively. Here the saddle-splay term is omitted because in the following we consider infinitely strong boundary conditions. Within this hypothesis, the saddle-splay term, which is a null Lagrangian [6], does not affect the equilibrium configurations.

In the presence of an electric field \mathbf{E} , the free-energy density acquires an additional term describing the field-matter interaction [1]

$$w_{int} = -\frac{\epsilon_a}{2}(\mathbf{n} \cdot \mathbf{E})^2, \quad (1)$$

where ϵ_a denotes the dielectric anisotropy. In the following we restrict our attention to $\epsilon_a > 0$.

Let us introduce a set of cylindrical coordinates (r, θ, z) , centered in O . We also let $\{\mathbf{e}_r, \mathbf{e}_\theta\}$ be unit vectors pointing in the radial and azimuthal directions, respectively. Let us assume that the nematic occupies the region between two infinite concentric cylinders: $\Omega \equiv \{(r, \theta, z) | R \leq r \leq \rho R, 0 \leq \theta < 2\pi, -\infty < z < \infty\}$ with $R > 0$. The equilibrium configurations of the nematic are extremal points of the total energy functional

$$\mathcal{F} = \int_{\mathcal{D}} (w_N + w_{int}) dv, \quad (2)$$

according to the imposed boundary conditions.

In practice, delimiting walls can be treated in such a way to induce a specific orientation of the molecules on the boundary, that is

$$\mathbf{n}(r=R) = \mathbf{n}(r=\rho R) = \mathbf{e}_z. \quad (3)$$

It is worth noticing that, in the absence of an applied electric field, the energy functional reaches the absolute minimum whenever \mathbf{n} is uniform in the sample. Once taking into account the boundary conditions (3), we deduce that, in the field-free configuration, the director field $\mathbf{n} = \mathbf{n}_0$ is uniformly aligned in the \mathbf{e}_z direction.

Let V denote the applied voltage between the outer and the inner domain delimiting surfaces. The electrostatic potential ϕ satisfies the Laplace equation $\Delta\phi=0$ that, together with the boundary condition $\phi(\rho R) - \phi(R) = V$, gives the electrostatic field in the radial direction

$$\mathbf{E} = -\frac{V}{r \ln \rho} \mathbf{e}_r, \quad R \leq r \leq \rho R. \quad (4)$$

Notice that the positiveness of dielectric anisotropy allows the molecules to prefer the radial alignment. On the contrary, the elastic forces together with the boundary conditions favor the \mathbf{n}_0 alignment. Given the results for planar samples, we expect a critical value of the voltage strength beyond which the uniform solution bifurcates and a static distortion occurs.

It should be stressed that our analysis is restricted to the so called *magnetic approximation* [19]: the electric field induces reorientation of the molecules, but it is not affected by distortion of the nematic director. A detailed discussion of this point is presented in Appendix A.

By analogy with the planar case, we assume that the field-induced director distortions are homogeneous along the direction of the unperturbed alignment, hence we look for configurations described by $\mathbf{n}(r, \theta)$. This allows to restrict our study to an arbitrary orthogonal cross section B of the domain \mathcal{D} and, therefore, to deal with the functional

$$\mathcal{W} = \int_B (w_N + w_{int}) r dr d\theta, \quad (5)$$

where B denotes the planar annular region $B = \{(r, \theta) | R \leq r \leq \rho R, 0 \leq \theta < 2\pi\}$.

We parametrize the nematic director by the angles $\alpha(r, \theta)$ and $\eta(r, \theta)$ such that

$$\mathbf{n} = \sin \alpha \mathbf{e}_r + \cos \alpha \sin \eta \mathbf{e}_\theta + \cos \alpha \cos \eta \mathbf{e}_z.$$

Thus, the undistorted configuration $\mathbf{n}_0 = \mathbf{e}_z$ is represented by

$$\alpha = \alpha_0 = 0, \quad \eta = \eta_0 = 0, \quad \forall r \in [R, \rho R], \quad \forall \theta \in [0, 2\pi).$$

In order to assess the critical threshold, we consider small perturbations of the initial configuration \mathbf{n}_0 . By setting

$$\alpha = \alpha_1(r, \theta), \quad \eta = \eta_1(r, \theta), \quad \alpha_1, \eta_1 \ll 1$$

we expand the free energy [Eq. (5)] in Taylor series of the variables α_1 and η_1 . Up to the quadratic order, the energy functional becomes

$$W = K_1 \int_0^{2\pi} d\theta \int_R^{\rho R} dr \left[\frac{1}{2r} \left(\alpha_1 + r \frac{\partial \alpha_1}{\partial r} + \frac{\partial \eta_1}{\partial \theta} \right)^2 + \frac{\kappa}{2r} \left(\eta_1 + r \frac{\partial \eta_1}{\partial r} - \frac{\partial \alpha_1}{\partial \theta} \right)^2 - \frac{v^2 \alpha_1^2}{2r \ln^2 \rho} \right], \quad (6)$$

where we have introduced the elastic anisotropy κ and the dimensionless applied potential v defined by

$$\kappa = \frac{K_2}{K_1}, \quad v = V \sqrt{\frac{\epsilon_a}{K_1}}.$$

Since the free energy involves only the square of v , in the following only positive values of v are considered, without loss of generality. In fact, the negative counterpart corresponds to the physical symmetric problem wherein the electric field vector reverses sign. In the next two sections we provide the analysis of the linearized equilibrium equations for purely radial and θ -periodical field-induced director distortions.

III. HOMOGENEOUS FREEDERICKSZ TRANSITION

By analogy with the planar case, the simplest expected field-induced distortion is purely radial. Hence, let us suppose that α_1 and η_1 do not depend on θ . The free-energy [Eq. (6)] becomes

$$W_r = 2\pi K_1 \int_R^{\rho R} \left[\frac{1}{2r} \left(\alpha_1 + r \frac{d\alpha_1}{dr} \right)^2 + \frac{\kappa}{2r} \left(\eta_1 + r \frac{d\eta_1}{dr} \right)^2 - \frac{v^2 \alpha_1^2}{2r \ln^2 \rho} \right] dr,$$

that leads to the following Euler-Lagrange equations:

$$r^2 \frac{d^2 \alpha_1}{dr^2} + r \frac{d\alpha_1}{dr} + [v^2 (\ln \rho)^{-2} - 1] \alpha_1 = 0, \quad (7a)$$

$$r^2 \frac{d^2 \eta_1}{dr^2} + r \frac{d\eta_1}{dr} - \eta_1 = 0. \quad (7b)$$

Accordingly to the boundary conditions (3), the unknown fields possess vanishing boundary values

$$\alpha_1(R) = \alpha_1(\rho R) = 0, \quad \eta_1(R) = \eta_1(\rho R) = 0.$$

Equations (7) can be transformed in a system of linear ordinary differential equations with constant coefficients by putting

$$r = Re^y \rightarrow \begin{cases} r \frac{d}{dr} = \frac{d}{dy} \\ r \frac{d}{dr} r \frac{d}{dr} = r^2 \frac{d^2}{dr^2} + r \frac{d}{dr} = \frac{d^2}{dy^2}. \end{cases} \quad (8)$$

Indeed, by defining $\bar{\alpha}(y) = \alpha_1(Re^y)$ and $\bar{\eta}(y) = \eta_1(Re^y)$ Eqs. (7) transform respectively in

$$\bar{\alpha}'' + [v^2 (\ln \rho)^{-2} - 1] \bar{\alpha} = 0, \quad (9a)$$

$$\bar{\eta}'' - \bar{\eta} = 0, \quad (9b)$$

where a prime denotes differentiation with respect to y . These equations must be solved together with the boundary conditions

$$\bar{\alpha}(0) = \bar{\alpha}(\ln \rho) = 0, \quad (10a)$$

$$\bar{\eta}(0) = \bar{\eta}(\ln \rho) = 0. \quad (10b)$$

Equation (9b), together with the boundary conditions (10b), yields $\eta_1(r) = 0$. This means that the distorted director field lies in the plane spanned by \mathbf{e}_r and \mathbf{e}_z (see Fig. 1 central panel).

Equation (9a) coupled with the boundary conditions (10a) gives an eigenvalue problem, whose non trivial solutions are in the form (C_1 is an undetermined parameter)

$$\bar{\alpha} = C_1 \sin\left(\frac{n\pi}{\ln \rho} y\right), \quad 0 \leq y \leq \ln(\rho), \quad (11)$$

provided that the dimensionless applied voltage v complies with the second degree equation

$$v_{(n)}^2 = n^2 \pi^2 + \ln^2 \rho, \quad (12)$$

where $n \neq 0$ is an integer. The critical threshold v_c for the HFT is the minimum value among those given $v_{(n)}$, which is indeed retrieved at $n = \pm 1$

$$v_c = \sqrt{\pi^2 + \ln^2 \rho}. \quad (13)$$

The same result has been obtained by Barratt and Duffy (see the Case VI discussed in the Sect 4.1 of [18]). The critical applied voltage for the planar case $v_c = \pi$ is recovered in the limit $\rho \rightarrow 1^+$.

IV. PERIODIC FREEDERICKSZ TRANSITION

Up to this point, we have studied the special class of solutions which depend only on the radial coordinate. In this

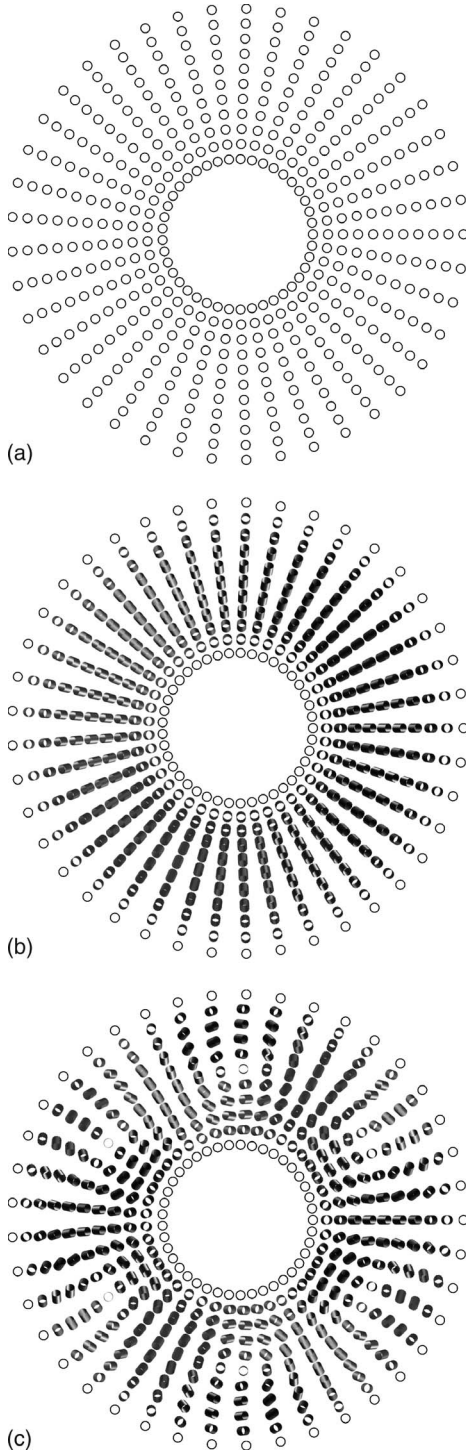


FIG. 1. Schematic representation of Fréedericksz transitions for a nematic confined between two concentric cylinders, when a radial electric field is applied. The vector field \mathbf{n} is portrayed in a right section of the domain. Top: field-free configuration. Strong planar boundary conditions impose an uniform alignment of the molecules along the cylinder axis. Center: HFT. The director field results distorted: the molecules rotate the plane spanned \mathbf{e}_r and \mathbf{e}_z , maintaining zero their azimuthal component. Bottom: PFT. The molecules undergo a spatial distortion which is periodic in the azimuthal direction. The director is plotted according to our numerical solution (see Fig. 5) and it is worth noticing the close resemblance with the path reported in Fig. 1 of [14].

section we analyze solutions depending on both the radial and the tangential coordinates. By analogy with the case reported in [7], we expect that the nematic director undergoes a periodic distortion in the \mathbf{e}_θ direction. Let us consider periodic solutions in the form

$$\alpha_1 = \varphi(r)\cos(q\theta), \quad \eta_1 = \gamma(r)\sin(q\theta), \quad (14)$$

with q integer. The number q plays a similar role of the undulation wave vector in the planar case. For $q=0$ we recover the case discussed in the previous section.

We insert Eq. (14) into Eq. (6) and we integrate over θ obtaining

$$\begin{aligned} W_p = K_1 \pi \int_R^{\rho R} \left\{ \frac{1}{2} \left[\left(\frac{d\varphi}{dr} \right)^2 + \kappa \left(\frac{d\gamma}{dr} \right)^2 \right] + \frac{1}{r} \left[\kappa(q\varphi + \gamma) \frac{d\gamma}{dr} \right. \right. \\ \left. \left. + (q\gamma + \varphi) \frac{d\varphi}{dr} \right] + \frac{1}{2r^2} [(\kappa q^2 + 1)\varphi^2 + 2q(\kappa + 1)\varphi\gamma \right. \\ \left. + (\kappa + q^2)\gamma^2] - \frac{v^2 \varphi^2}{2r^2 \ln^2 \rho} \right\} r dr. \end{aligned} \quad (15)$$

The Euler-Lagrange equations associated to the functional (15) are two coupled linear ordinary differential equations of the second order

$$\begin{aligned} r^2 \frac{d^2 \varphi}{dr^2} + r \frac{d\varphi}{dr} - (1 + \kappa q^2)\varphi + r q(1 - \kappa) \frac{d\gamma}{dr} - (1 + \kappa)q\gamma \\ + (\ln \rho)^{-2} v^2 \varphi = 0, \end{aligned} \quad (16a)$$

$$\kappa \left(r^2 \frac{d^2 \gamma}{dr^2} + r \frac{d\gamma}{dr} \right) - (\kappa + q^2)\gamma + r q(\kappa - 1) \frac{d\varphi}{dr} - (1 + \kappa)q\varphi = 0. \quad (16b)$$

The boundary conditions (3) allow to deduce the boundary values:

$$\varphi(R) = \varphi(\rho R) = 0, \quad \gamma(R) = \gamma(\rho R) = 0. \quad (16c)$$

In order to make the problem more tractable, we again perform the transformation (8). By defining $\zeta \equiv v/\ln \rho$, $\bar{\varphi}(y) = \varphi(Re^y)$ and $\bar{\gamma}(y) = \gamma(Re^y)$ a system of linear differential equations with constant coefficients is obtained

$$\bar{\varphi}'' - (1 + \kappa q^2 - \zeta^2)\bar{\varphi} + q(1 - \kappa)\bar{\gamma}' - (1 + \kappa)q\bar{\gamma} = 0, \quad (17a)$$

$$\kappa \bar{\gamma}'' - (\kappa + q^2)\bar{\gamma} + q(\kappa - 1)\bar{\varphi}' - (1 + \kappa)q\bar{\varphi} = 0, \quad (17b)$$

that can be solved by standard methods. Indeed, putting

$$X = \begin{pmatrix} \bar{\varphi} \\ \bar{\varphi}' \\ \bar{\gamma} \\ \bar{\gamma}' \end{pmatrix} \quad (18)$$

the Eqs. (17) are reduced to the first order problem

$$X(y)' = A X(y), \quad (19)$$

where the matrix A is

$$A = \begin{pmatrix} 0 & 1 & 0 & 0 \\ 1 + \kappa q^2 - \zeta^2 & 0 & (1 + \kappa)q & -(1 - \kappa)q \\ 0 & 0 & 0 & 1 \\ \frac{1 + \kappa}{\kappa}q & \frac{1 - \kappa}{\kappa}q & \frac{\kappa + q^2}{\kappa} & 0 \end{pmatrix}. \quad (20)$$

The eigenvalues of A can be found from the characteristic equation $p(\sigma) = \det(A - \sigma I)$ and are the roots of the quartic polynomial

$$p(\sigma) = \sigma^4 - [2(1 + q^2) - \zeta^2]\sigma^2 - [\zeta^2(\kappa + q^2)\kappa^{-1} - (1 - q^2)^2] = 0. \quad (21)$$

and can be written as

$$\sigma^2 = 1 + q^2 - \frac{\zeta^2}{2} \mp \sqrt{\frac{\zeta^4}{4} + 4q^2 + q^2 \frac{1 - \kappa}{\kappa} \zeta^2} = f_{q^{\pm}}, \quad (22)$$

A rapid inspection shows that substituting $q=0$ one gets the solutions of Eq. (11) with the values [Eq. (13)] of the critical field; moreover the matrix A becomes block diagonal thus decoupling the equation for $\bar{\varphi}$ from that of $\bar{\gamma}$. For $q \neq 0$ it follows that the solution can be written as a linear combination of $\sinh(\omega_+ y)$, $\cosh(\omega_+ y)$, $\sinh(\omega_- y)$, and $\cosh(\omega_- y)$, where $\omega_+ = \sqrt{f_{q^+}}$ and $\omega_- = \sqrt{f_{q^-}}$. Special care must be payed when $\zeta = (q^2 - 1)\sqrt{\kappa(\kappa + q^2)^{-1}}$ because $\omega_- = 0$ and the solution is a linear combination of $\sinh(\omega_+ y)$, $\cosh(\omega_+ y)$, 1 and y . Therefore, for convenience we prefer to have an expression which is valid for all values of ζ and, thus, it is better to write the solution in term of the exponential matrix

$$X(y) = e^{A y} X(0) = B(y) X(0). \quad (23)$$

The explicit expression of $e^{A y}$ is given in the Appendix B.

The ‘‘initial values’’ vector $X(0)$ contains four arbitrary constants which are at disposal to satisfy the boundary conditions,

$$\bar{\varphi}(0) = \bar{\varphi}(\ln \rho) = 0, \quad \bar{\gamma}(0) = \bar{\gamma}(\ln \rho) = 0. \quad (24)$$

Letting $X(0) = (C_1, C_2, C_3, C_4)^t$ it easily follows that $C_1 = C_3 = 0$ satisfies the boundary conditions at $y=0$. The boundary conditions at $y = \ln \rho$ lead to the linear system

$$\begin{pmatrix} B(\ln \rho)_{1,2} & B(\ln \rho)_{1,4} \\ B(\ln \rho)_{3,2} & B(\ln \rho)_{3,4} \end{pmatrix} \begin{pmatrix} C_2 \\ C_4 \end{pmatrix} = M \begin{pmatrix} C_2 \\ C_4 \end{pmatrix} = 0. \quad (25)$$

Nontrivial solutions for C_2 and C_4 can be found if and only if

$$\det M \equiv G(\kappa, q, \ln \rho, v) = 0. \quad (26)$$

The explicit expression for the highly nonlinear function $G(\kappa, q, \ln \rho, v)$ is reported in Appendix B. Here we simply report its graph in a particular case (see Fig. 2). Similar graphs are encountered for different parameters values.

As can be seen in Fig. 2, the values of v at which $G=0$ form a discrete set at which PFT can occur. In the following we are interested only in those solutions of Eq. (26) for v which are less than v_r . When this set is not empty, the smallest among its elements defines the critical threshold v_{cr} for the PFT (see below for more details). In the planar geometry,

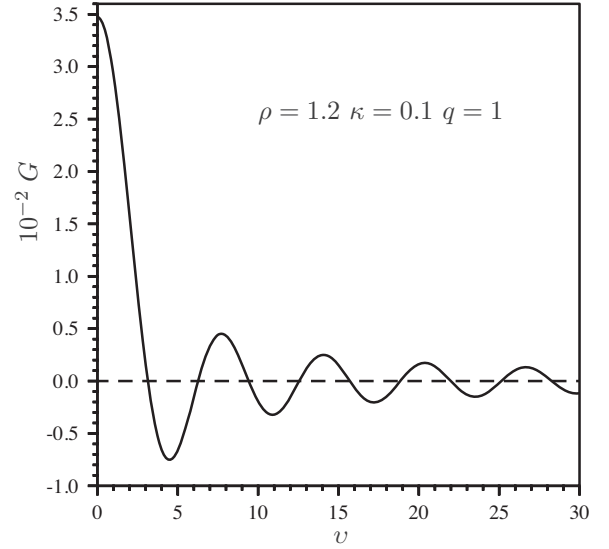


FIG. 2. The determinant G as a function of v .

PFT occurs only for values of κ less than the critical value $\kappa_{pl} = 0.30325$. In the next section, we show that in the annular geometry the upper limit κ_{cr} for the existence of the PFT is an increasing function of ρ , which in the planar limit ($\rho \rightarrow 1^+$) attains its minimum $\kappa_{cr} = \kappa_{pl}$.

V. RESULTS

In order to assess the critical threshold as a function of κ and ρ , we have numerically evaluated the roots of Eq. (26). More precisely, for each value of ρ , κ and $q \geq 0$, we look for the smallest solution v_0 of Eq. (26). In this manner, we numerically obtain a function $v_0 = v_0(\rho, \kappa, q)$. This function starts at $q=0$ with v_r , that is $v_0(\rho, \kappa, 0) \equiv v_r$. Then as q increases v_0 decreases reaching a minimum and eventually increases. The thus-obtained minimum defines the critical threshold $v_{cr}(\kappa, \rho)$ and the corresponding value of q , denoted with $q_{cr}(\kappa, \rho)$, defines the number of stripes that appear at the critical threshold. In Fig. 3 is shown the behavior of v_{cr} and q_{cr} as a function of κ for different values of ρ .

To better discuss our results, it is worthwhile to remark that values of ρ close to unity describe thin samples, while higher values of ρ define the thick cell regime. In fact, the aspect ratio μ of our domain, defined as the ratio between the mean circumference and the thickness of the sample,

$$\mu = \frac{\pi(\rho + 1)}{\rho - 1} \quad (27)$$

becomes very large as $\rho \rightarrow 1^+$. Conversely, μ reaches its minimum π as $\rho \rightarrow \infty$.

The behavior of the critical threshold v_{cr} as a function of κ for several values of ρ is reported in Fig. 3(a). Each curve consists of an increasing part, in correspondence of which PFT occurs, and a plateau zone which denotes of a range of κ values where homogeneous transition occurs. The beginning of the plateau zone corresponds in Fig. 3(b) to the transition from the critical mode $q_{cr} = 1$ to the critical mode $q_{cr} = 0$. For a fixed values of ρ there exists a critical value of κ ,

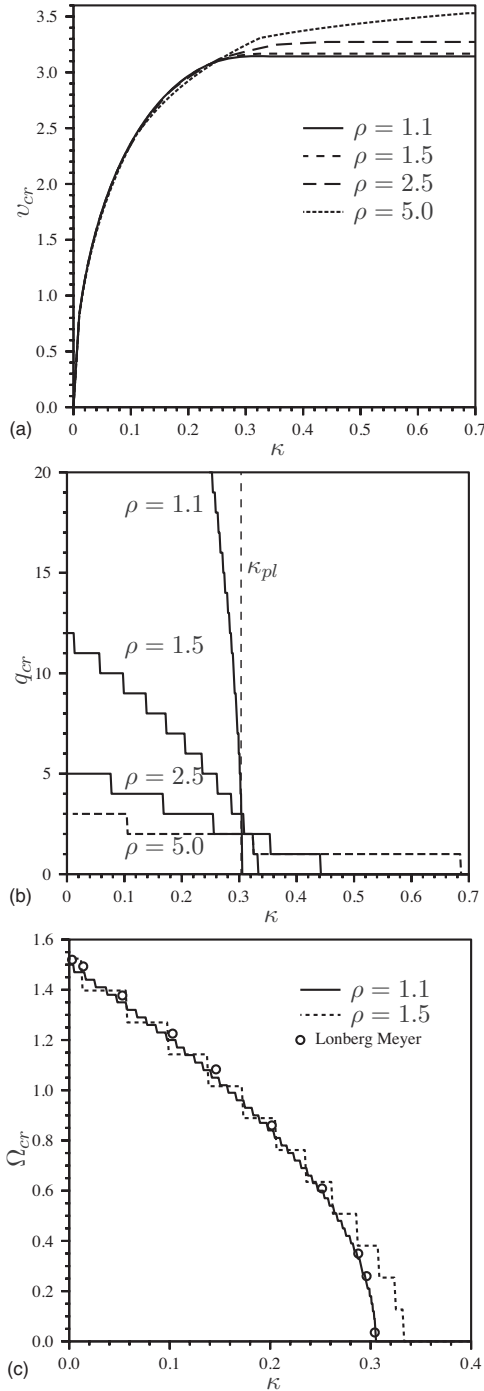


FIG. 3. The critical threshold v_c (top), the critical undulation wave number (center) as a function of κ for different values of ρ . In the bottom is shown a comparison with the Lonberg and Meyer results (see text).

denoted by κ_{cr} , below of which PFT occurs. In very thin cells, i.e., in the limit $\rho \rightarrow 1^+$, κ_{cr} approaches its minimum value that coincides with κ_{pl} . Furthermore, κ_{cr} is an increasing function of ρ . This has a very remarkable consequence: the PFT, that in the planar case is observable in nematic with very large elastic anisotropy, in annular geometry can also occur for usual nematic, provided that thick samples are considered.

As κ tends toward zero, the only admissible distortion is pure twist. Within this limit we have seen that the critical field tends to zero as $\sqrt{\kappa}$. In Fig. 3(b) the optimal wave number at the critical threshold is reported. For small values of κ the number of stripe domains increases. Indeed, the twist mode becomes more and more energetically preferred as κ decreases. However, the presence of the walls bounds from above the wave number: in the limit $\kappa \rightarrow 0$ the width of a single stripe is of the same order of magnitude of the cell thickness. For a given ρ the critical wave number is a non-increasing piece-wise function of κ . Thus, for increasing values of κ the undulation spreads more and more on the entire domain, reaching the pure splay configuration at κ_{cr} .

In Fig. 3(c) a comparison of our results with those of Lonberg and Mayer [their Fig. 3(b)] is performed. In [7] the authors denotes q the in-plane wave vector measured in unit of $\pi/\text{thickness}$. The quantity to compare with is $\Omega_{cr} = 2q_{cr}/\mu$, where μ is the aspect ratio [defined by formula (27)]. In particular when $\rho = 1.1$ and κ tends to zero Ω_{cr} is very close to 1.51, thus easily verifying that in the thin cell regime ($\rho \approx 1$) both results are comparable.

The rate of spreading of the undulation depends on ρ . Thus, in the thick cell regime transition between different modes seems to occur in bursts. Conversely, in the thin cell regime the mode change becomes more and more continuous as $\rho \rightarrow 1^+$. This suggests that in the thin cell regime the transition from PFT to HFT, when the control parameter is κ , is a second order phase transition. Consequently, we can adopt the arguments pursued in [11] to obtain some analytical estimation for κ_{cr} .

Let us introduce the dimensionless parameter

$$\xi = \frac{q}{v} \ln \rho \quad (28)$$

and we set $v_{cr} = v_r(1 + \beta\xi^2)$. We expand Eq. (26) up to $O(\xi^2)$ and then we solve for β obtaining

$$\beta = \frac{a\kappa^2 - 2[b(\ln^2 \rho + \pi^2)v_r^2 - a]\kappa - bv_r^4 + a}{v_r b \kappa}, \quad (29)$$

where

$$a = 4\pi^2(1 + \rho)\ln \rho, \quad b = \rho - 1.$$

The existence of negative values of β ensures that the $v_{cr} < v_r$, and therefore that the periodic Fréedericksz transition occurs. Notice that the denominator of the right hand side of Eq. (29) is positive. Since $a > 0$, negative values of β are attained for $\kappa \in (\kappa_-, \kappa_+)$, being κ_- and κ_+ roots of numerator of Eq. (29), such that $\kappa_- < \kappa_+$. A direct inspection of the solutions leads to $\kappa_- < 0$ and $\kappa_+ > 0$ for all ρ . Then, for a given ρ , PFT occurs for $\kappa \in (0, \kappa_+]$.

Figure 4 reports the comparison between the numerical κ_{cr} and the analytical one that coincides with κ_+ . The two graphs agree in the regime of thin cells where the parameter ξ is very small. The mismatch at high values of ξ is of $O(\xi^3)$.

Notice that, in the limit $\rho \rightarrow 1^+$ Eq. (29) reduces to Oldano's formula [11]

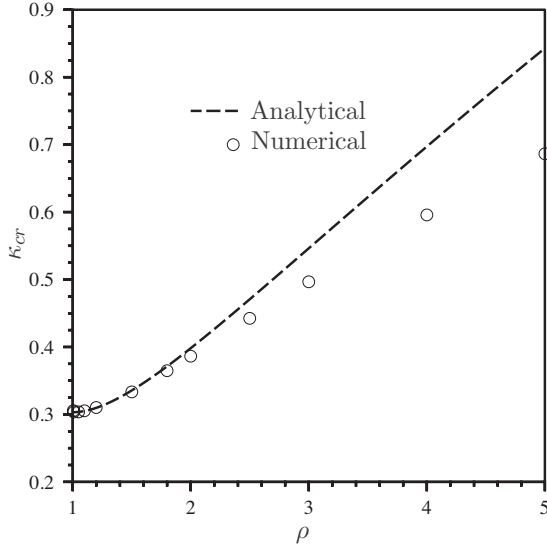


FIG. 4. Critical κ as a function of ρ . The dashed curve is given by the formula (29)

$$\beta = \frac{4}{\pi^2 \kappa} \left[\kappa^2 + (2\kappa - 1) \left(\frac{\pi^2}{8} - 1 \right) \right], \quad (30)$$

that yields the critical value of κ_{pl} for the planar geometry.

Typical solution shape are displayed in Fig. 5. Remark that, with respect to the planar case, the solutions lose their symmetry with respect to center of the cell. In particular, the maximum of $\bar{\varphi}$ and the zero of $\bar{\gamma}$ turn out to be displaced toward the outer delimiting wall.

VI. CONCLUDING REMARKS

It has been shown that the periodical splay-twist Fréedericksz transition is theoretically possible for nematic confined in the region between two infinite concentric cylinders,

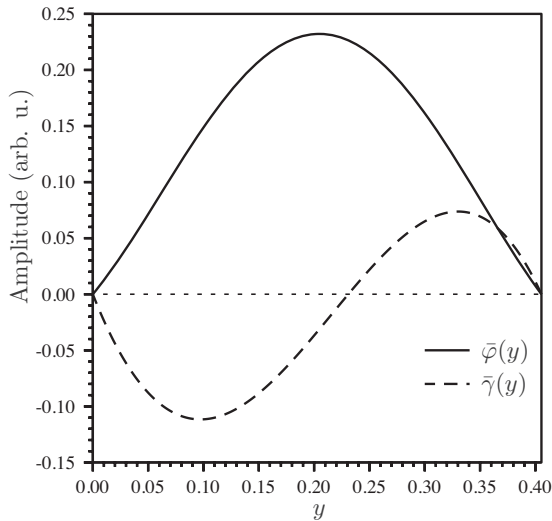


FIG. 5. An example of numerical solution for $\bar{\varphi}(y)$ and $\bar{\gamma}(y)$ [see Eqs. (17)]. The parameters are $\kappa=0.2$, $\rho=1.5$, $q=7$, and the critical voltage numerically found $v_c \approx 2.965886$.

where the molecules are initially aligned along the domain symmetry axis. An applied voltage between the delimiting walls generates a radial electric field that is able to induce homogeneous or periodic distortions of the director in the azimuthal direction. For the HFT the results of [18] are recovered, while for the PFT, the threshold given by a transcendental equation, has been evaluated numerically and it turns out that it depends on the elastic anisotropy κ , and ρ , the ratio between the outer and the inner radii of the delimiting cylinders. As expected, in the limit of very thin samples ($\rho \rightarrow 1^+$) the resulting threshold matches the value of the planar case.

The theory for the planar samples predicts that splay-twist PFT transition occurs only in polymeric liquid crystal, where $K_2/K_1 < \kappa_{pl}$. On the contrary, as a result of our analysis, cylindrical samples allow the PFT also in common nematics contained in thick cells. For example, the splay and the twist Frank's constants for 5CB (4'-n-pentyl-4-cyanobiphenyl) at 24 °C [20] are

$$K_1 = 6.1 \times 10^{-7} \text{ dyn} \quad K_2 = 3.1 \cdot 10^{-7} \text{ dyn},$$

respectively. For this nematic liquid crystal is not possible to observe PFT in the planar case, because $\kappa=0.51 > \kappa_{pl}$. On the contrary, if we consider a cylindrical domain with $\rho=5$, our analysis predicts (see Fig. 3) that the PFT can occur and the undulation wavelength is of the order of the mean radius.

This effect could be useful, for instance, for the measurement of elastic constants. Future developments can be pursued along three directions. One can extend our results, by dealing with the same geometry domain considering different initial alignment of the molecules and electric field (mutually orthogonal). Notice that the radial and the azimuthal initial configurations are already distorted states and instability can be induced in field-free configuration by simply reducing the radius of the inner cylinder. By analogy with the HFT [15], one could expect that the threshold becomes infinitesimal by increasing ρ .

Another generalization of this work could include the influence of weak anchoring boundary conditions. In this case the saddle-splay term of the Frank energy is expected to play a role in the balance of boundary actions and experimental measurement of v_c may provide more information on the K_{24} constant.

Finally, it could be interesting to explore the equilibrium configuration for high applied fields. In the light of the experimental [14] and numerical results [21] for the planar case, one might expect that at high fields the periodic structure is replaced again by the purely radial solution. The analysis in this regime involves nonlinear partial differential equations that can be approached via numerical techniques.

APPENDIX A: THE MAGNETIC APPROXIMATION

In this Appendix we discuss the case of complete field-matter coupling. Following Deuling [22] the field-matter free-energy density is

$$w_{int} = -\frac{1}{2} \mathbf{D} \cdot \mathbf{E}, \quad (\text{A1})$$

instead of Eq. (1), where $\mathbf{D} = \epsilon_{\perp} \mathbf{E} + \epsilon_a (\mathbf{n} \cdot \mathbf{E}) \mathbf{n}$ represents the dielectric displacement. The parameter ϵ_{\parallel} and ϵ_{\perp} are the static dielectric constants measured along or normal to the molecular axis. The quantity $\epsilon_a = \epsilon_{\parallel} - \epsilon_{\perp}$ measures the dielectric anisotropy.

Equation (A1) can be express in terms of the electric field as

$$w_{int} = -\frac{\epsilon_{\perp}}{2} \mathbf{E}^2 - \frac{\epsilon_a}{2} (\mathbf{n} \cdot \mathbf{E})^2. \quad (\text{A2})$$

Notice that, if one thinks that \mathbf{E} is assigned, Eq. (A2) reduces to Eq. (1) up to an inessential constant; otherwise, \mathbf{E} should be treated as an additional degree of freedom in the variation of the free energy.

Let ϕ denote the electrostatic potential so that $\mathbf{E} = -\nabla \phi$. It satisfies the boundary condition

$$\phi(\rho R) - \phi(R) = V. \quad (\text{A3})$$

In the undistorted configuration, but in the presence of an applied voltage, the total free energy reduces to

$$W_0 = -\frac{\epsilon_{\perp}}{2} \int_0^{2\pi} d\theta \int_R^{\rho R} |\nabla \phi|^2 r dr,$$

whose Euler-Lagrange equations is the Laplace equation $\Delta \phi = 0$ that together with the boundary condition (A3) yields the radial electrostatic field [Eq. (4)].

When the complete coupling holds, the description of slightly distorted configurations requires, in addition to η_1 and α_1 , a state variable describing the perturbation of the electric field with respect to radial solution (4). Thus, we set

$$\nabla \phi = -\mathbf{E}_0 + \nabla \phi_1, \quad (\text{A4})$$

where \mathbf{E}_0 is given by Eq. (4), while $\phi_1(r, \theta)$ is of the same order of $\alpha_1(r, \theta)$ and $\eta_1(r, \theta)$. More precisely, inasmuch Fréedericksz transition is a second order phase transition driven by the applied potential V , said ε^2 the relative difference between the applied voltage and the critical threshold, then α_1 , η_1 , and ϕ_1 must be $O(\varepsilon)$. Consequently, we deduce that ϕ_1 satisfies homogeneous boundary conditions,

$$\phi_1(R) = \phi_1(\rho R) = 0. \quad (\text{A5})$$

The excess of free-energy due to the distortion is

$$W = K_1 \int_0^{2\pi} d\theta \int_R^{\rho R} dr \left[\frac{1}{2r} \left(\alpha_1 + r \frac{\partial \alpha_1}{\partial r} + \frac{\partial \eta_1}{\partial \theta} \right)^2 + \frac{\kappa}{2r} \left(\eta_1 + r \frac{\partial \eta_1}{\partial r} - \frac{\partial \alpha_1}{\partial \theta} \right)^2 - \frac{v^2 \alpha_1^2}{2r \ln^2 \rho} - \frac{\epsilon_{\perp}}{K_1} r |\nabla \phi_1|^2 \right], \quad (\text{A6})$$

that differs from Eq. (6) just by the last term. Since in this term the gradient of ϕ_1 appears uncoupled by the other state variables, we can readily conclude that the Euler-Lagrange equation related to ϕ_1 is still the Laplace equation $\Delta \phi_1 = 0$, that solved with boundary conditions (A5) gives $\phi_1 = 0$ everywhere. According to this result, we can state that the criti-

cal threshold, whose calculation deals with the stationarity of Eq. (A6), is not affected by the complete field-matter coupling. This allows to justify the magnetic approximation assumed in Sec. II. However, we would to emphasize that the orthogonality between \mathbf{E}_0 and \mathbf{n}_0 is crucial in our calculation. Without this condition the linearized Euler-Lagrange equations do not decouple from each other. A counterexample is given in [23].

Even in our geometry, the equation may be couple at the quadratic order. This can affect the amplitude of the solutions close to the bifurcation point as outlined in [19,24] for the planar case. In this paper we just focus on critical threshold calculation, without determine the solutions amplitude that generally involves in higher order approximation of the free energy.

APPENDIX B: THE EXPONENTIAL MATRIX

The Cayley-Hamilton theorem states that substituting the matrix A in its characteristic polynomial results in the zero matrix,

$$A^4 = c_2 A^2 + c_0, \quad (\text{B1})$$

where the c_i can be read from Eq. (21). This means that each power A^n $n \geq 4$ can be expressed as a linear combination of $A^0 = \mathbb{1}$, A , A^2 , and A^3 . Let us concentrate first on the even powers. It can be easily shown that

$$A^{2n} = a_n A^2 + b_n \mathbb{1}, \quad (\text{B2})$$

with

$$\begin{cases} a_{n+1} = c_2 a_n + b_n \\ a_0 = 0 \end{cases} \quad \begin{cases} b_{n+1} = c_2 a_n \\ b_0 = 1 \end{cases}, \quad (\text{B3})$$

whose solution is

$$a_n = N(\omega_+^{2n} - \omega_-^{2n}),$$

$$b_n = N[(\omega_+^2 - c_2)\omega_+^{2n} - (\omega_-^2 - c_2)\omega_-^{2n}]. \quad (\text{B4})$$

with $N = (\omega_+^2 - \omega_-^2)^{-1}$. The odd powers show the same structure, namely, $A^{2n+1} = a_n A^3 + b_n A$. Next substituting these findings in the definition of exponential one finds

$$\begin{aligned} e^{Ay} &= \sum_{n=0}^{\infty} \frac{y^{2n}}{(2n)!} A^{2n} + \sum_{n=0}^{\infty} \frac{y^{2n+1}}{(2n+1)!} A^{2n+1} \\ &= \left[\sum_{n=0}^{\infty} \frac{y^{2n}}{(2n)!} b_n \right] \mathbb{1} + \left[\sum_{n=0}^{\infty} \frac{y^{2n}}{(2n)!} a_n \right] A^2 \\ &\quad + \left[\sum_{n=0}^{\infty} \frac{y^{2n+1}}{(2n+1)!} b_n \right] A + \left[\sum_{n=0}^{\infty} \frac{y^{2n+1}}{(2n+1)!} a_n \right] A^3 \\ &= N[f_0(y)\mathbb{1} + f_1(y)A + f_2(y)A^2 + f_3(y)A^3]. \end{aligned} \quad (\text{B5})$$

Using the explicit expressions of the a_n and b_n the series can be summed to

$$f_0(y) = (\omega_+^2 - c_2) \cosh(\omega_+ y) - (\omega_-^2 - c_2) \cosh(\omega_- y),$$

$$f_1(y) = \frac{\omega_+^2 - c_2}{\omega_+} \sinh(\omega_+ y) - \frac{\omega_-^2 - c_2}{\omega_-} \sinh(\omega_- y),$$

$$f_2(y) = \cosh(\omega_+ y) - \cosh(\omega_- y),$$

$$f_3(y) = \frac{1}{\omega_+} \sinh(\omega_+ y) - \frac{1}{\omega_-} \sinh(\omega_- y). \quad (\text{B6})$$

Calculating the determinant as stated above, one finds

$$G = N^2 \{ f_1(\ln \rho)^2 + q^2 (\kappa - 1)^2 \kappa^{-1} f_2(\ln \rho)^2$$

$$+ [(\kappa q^2 - 2q^2 - 1)\zeta^2 - (2\kappa q^2 - q^2 - 1)$$

$$\times (\kappa q^2 - 2q^2 + \kappa) \kappa^{-1}] f_3(\ln \rho)^2 + (c_2 - q^2 (\kappa - 1)^2 \kappa^{-1})$$

$$\times f_1(\ln \rho) f_3(\ln \rho) \}. \quad (\text{B7})$$

-
- [1] P. G. de Gennes and J. Prost, *The Physics of Liquid Crystals* (Clarendon Press, Oxford, 1993).
- [2] C. W. Oseen, *Trans. Faraday Soc.* **29**, 883 (1933).
- [3] H. Zocher, *Trans. Faraday Soc.* **29**, 945 (1933).
- [4] F. C. Frank, *Discuss. Faraday Soc.* **25**, 19 (1958).
- [5] V. Fréedericksz and V. Zolina, *Trans. Faraday Soc.* **29**, 919 (1933).
- [6] E. G. Virga, *Variational Theories for Liquid Crystals* (Chapman & Hall, 1994).
- [7] F. Lonberg and R. B. Meyer, *Phys. Rev. Lett.* **55**, 718 (1985).
- [8] M. F. Ledney, *JETP Lett.* **85**, 328 (2007).
- [9] U. A. Laudyn, A. E. Miroshnichenko, W. Krolikowski, D. F. Chen, Y. S. Kivshar, and M. A. Karpierz, *Appl. Phys. Lett.* **92**, 203304 (2008).
- [10] D. O. Krimer, *Phys. Rev. E* **79**, 030702 (2009).
- [11] C. Oldano, *Phys. Rev. Lett.* **56**, 1098 (1986).
- [12] W. Zimmermann and L. Kramer, *Phys. Rev. Lett.* **56**, 2655 (1986).
- [13] E. Miraldi, C. Oldano, and A. Strigazzi, *Phys. Rev. A* **34**, 4348 (1986).
- [14] G. Srajer, F. Lonberg, and R. B. Meyer, *Phys. Rev. Lett.* **67**, 1102 (1991).
- [15] D. R. M. Williams and A. Halperin, *Phys. Rev. E* **48**, R2366 (1993).
- [16] P. Cladys and M. Kleman, *J. Phys. (Paris)* **33**, 591 (1972).
- [17] P. J. Barratt and B. R. Duffy, *Liq. Cryst.* **19**, 57 (1995).
- [18] P. J. Barratt and B. R. Duffy, *J. Phys. D: Appl. Phys.* **29**, 1551 (1996).
- [19] C. P. Self, R. H. Please, and T. J. Sluckin, *Eur. J. Appl. Math.* **13**, 1 (2002).
- [20] J. D. Bunning, T. E. Faber, and P. L. Sherrell, *J. Phys. (France)* **42**, 1175 (1981).
- [21] D. Krzyżański and G. Derfel, *Phys. Rev. E* **61**, 6663 (2000).
- [22] H. Deuling, *Mol. Cryst. Liq. Cryst.* **19**, 123 (1972).
- [23] G. Bevilacqua and G. Napoli, *Phys. Rev. E* **72**, 041708 (2005).
- [24] G. Napoli, *J. Phys. A* **39**, 11 (2006).